**Artículo de investigación**

# Petrology, geochemistry and petrogenesis of intrusive rock units of Varcheh, SE Arak, Iran.

## Petrología, geoquímica y petrogénesis de unidadies de roca intrusivas de Varcheh, SE Arak, Irán.

## Petrologia, geoquímica e petrogênese de unidades de rochas intrusivas de Varcheh, SE Arak, Irã.

Recibido: 20 de septiembre de 2018. Aceptado: 11 de octubre de 2018

Written by:
Saeed Naeemi
Mohammad-Ali Arian*
Nader Kohansal-Ghadimvand
*Department of geology, faculty of science, North Tehran Branch, Islamic Azad University, Tehran, Iran*
Saeednaemi38@gmail.com
m_arian@iau-tb.ac.ir*
N_Kohansal_ghadimvand@iau-tnb.ac.ir

**Abstract**

The area covering south and southeast Arak toward north Khomein, there are several intrusive igneous rocks including gabbro and monzodiorite units. Intrusive units consists of gabbro to diorite. These intrusive units belong to tertiary period. Over 120 samples were collected from the outcrops and thin section studies and geochemical analysis were carried out as well. 14 samples have been sent for ICP and basic melt analysis for studying major and rare earth elements. The results are compiled by related software. As far as mineralogy is concerned, plagioclase, pyroxene (augite type) and orthoclase are the dominant minerals recognized in the samples. Petrological and mineralogical similarities among the studied samples may suggest a presence of a huge gabbro-diorite batholith between Arak and Khomein. The outcrops of this batholith can be seen in the studied area as a result of erosion. In the other word, some fingerprints of a huge batholite can be observed in the studied area.

**Keywords:** petrogenesis, geochemistry, tertiary intrusive rocks, Varcheh, Iran.

**Resumen**

El área que cubre el sur y sureste de Arak hacia el norte de Jomein, hay varias rocas ígneas intrusivas que incluyen unidades de gabbro y monzodiorita. Las unidades intrusivas consisten en gabbro a diorita. Estas unidades intrusivas pertenecen al período terciario. Se recolectaron más de 120 muestras de los afloramientos y se realizaron estudios de sección delgada y también se realizaron análisis geoquímicos. Se enviaron 14 muestras para ICP y análisis de fusión básico para estudiar elementos de tierras mayores y raras. Los resultados son compilados por software relacionado. En cuanto a la mineralogía, plagioclasa, piroxeno (tipo augita) y ortoclasa son los minerales dominantes reconocidos en las muestras. Las similitudes petrológicas y mineralógicas entre las muestras estudiadas pueden sugerir la presencia de un enorme batolito de diorita gabbro entre Arak y Jomein. Los afloramientos de este batolito se pueden ver en el área estudiada como resultado de la erosión. En otras palabras, se pueden observar algunas huellas dactilares de una batolita enorme en el área estudiada.

**Palabras claves:** petrogénesis, geoquímica, rocas intrusivas terciarias, Varcheh, Irán.

**Resumo**

A área que cobre o sul e sudeste de Arak em direção ao norte de Khomein, existem várias rochas ígneas intrusivas, incluindo unidades de gabro e monzodiorito. Unidades intrusivas consistem de gabro para diorito. Essas unidades intrusivas pertencem ao período terciário. Mais de 120 amostras foram coletadas

dos afloramentos e estudos de seção fina e análises geoquímicas também foram realizadas. 14 amostras foram enviadas para análise de ICP e fundição básica para estudar elementos de terras grandes e raras. Os resultados são compilados por software relacionado. Quanto à mineralogia, plagioclásio, piroxena (tipo augita) e ortoclásio são os minerais dominantes reconhecidos nas amostras. Semelhanças petrológicas e mineralógicas entre as amostras estudadas podem sugerir a presença de um enorme batólito de gabro-diorito entre Arak e Khomein. Os afloramentos deste batólito podem ser vistos na área estudada como resultado da erosão. Em outra palavra, algumas impressões digitais de um enorme batólito podem ser observadas na área estudada.

**Palavras-chave:** petrogênese, geoquímica, rochas intrusivas terciárias, Varcheh, Irã

## 1. Introduction

The studied area is located between the longitudes of 490 45' to 500 00' and the latitudes 33045' to 34000' located on 1:100K geological map of Varcheh (Figure 1 and 2). There are 30 small intrusive units in south and southeast Arak which their size varies from 0.5 to 5 km2.


Figure 1- Satellite map of the studied area (Google EarthImage landsat / Comernicus 2016)

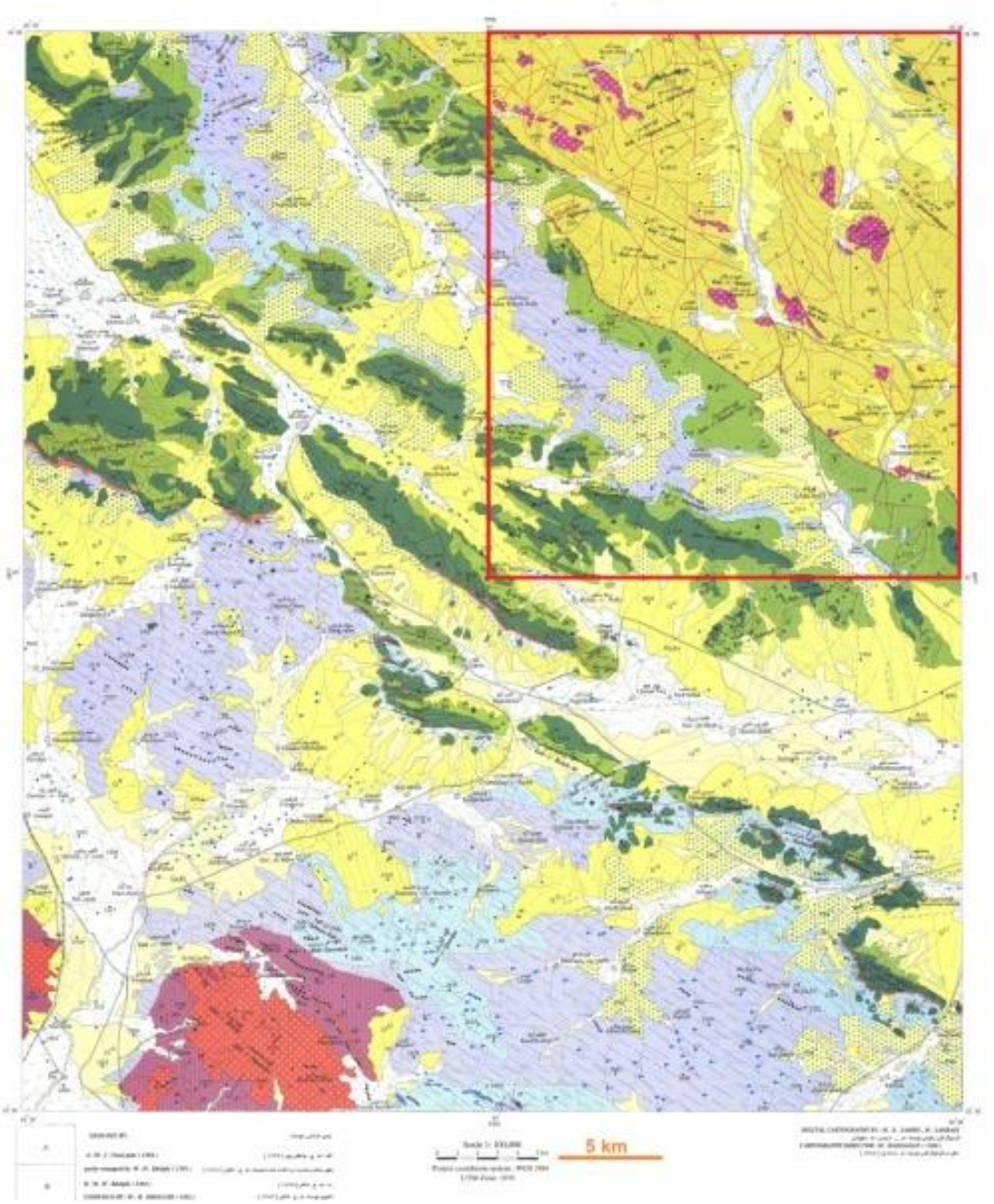


Figure 2- The studied area (Red rectangle) on 1:100K geological map of Varcheh (Geological Survey of Iran) (Vaezipour, 1985&Kholghi, 2004)

In the petrological point of view, the outcrops include a range of rocks from gabbro to diorite. The age of these outcrops are tertiary (based on the 1:100k geological map of Varcheh) which have entered to intermediate to upper cretaceous sedimentary rocks including limy shales, marl and siltstone.

Different rocks units with different genesis and ages lead to a different stratigraphy and geomorphology in a different parts of the studied area. Apart from rock type, reginal tectonic and volcanic activities also play a significant rule on the geomorphology of the studied area. This paper focuses on genesis and petrographic and petrological studies of the intrusive rocks of the studied area.

## 2. Geology

The studied area is a part of tectonic zone of Sanandaj-Sirjan volcanic belt which is one of the most active plates in Iran. According to significant massive volcanic rocks as well as progressive

development of metamorphic processes, Sanandaj-Sirjan volcanic belts is suggested as the most active region in Iran. Opening and closing of the young Tethys Ocean during Mesozoic period is considered as a responsible for activities in this region. In the other word, the tectonic plate is stemmed from a subduction and collision between the Arabian and Iran plates during late cretaceous to tertiary.

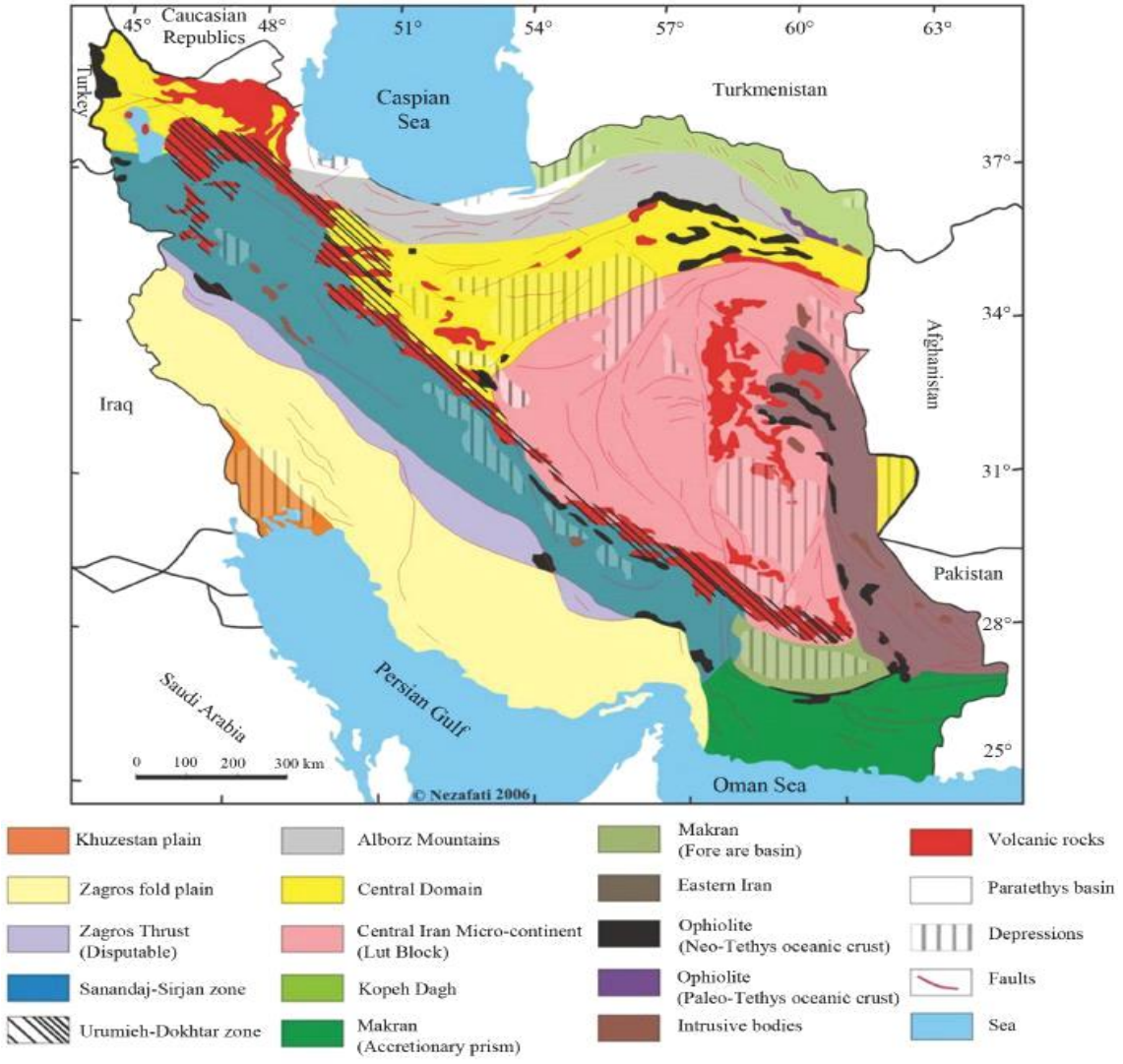


Figure 3- Geological zones of Iran and location of the studied area shown by white ellipsoid (Aghanabati, 2006)

Limestone rocks from bottom cretaceous in central and northern parts of the studied area are thicker and harder than the other outcrops observed in the area so that the highest elevations belong to the mentioned limestone rocks. These rocks have the same azimuth as the Zagros main direction which is NW-SE.

## 3. Materials and methods

Literature reviews were performed and related references were reviewed. Then, geological field trips and sampling processes were also carried out and thin section studies as well as petrographic studies (mineral type, texture, rocks ...) and ICP-MS analysis were performed. Newpet, and GCKIT software is used for interpreting the geochemical database. Also, related graphic and editing software (e.g.

Photoshop, Excel, Word and PowerPoint) is widely used for preparing the article.

### 3.1 Petrography

The rock units include fine to average grain gabbro, pyroxene gabbro, gabbro- diorite, diorite gabbro, pyroxene diorite, diorite, loco-diorite, and monzodiorite.

- Fine to coarse grain gabbro

Medium grained gabbro has grain and poikililtic texture. The main minerals are plagioclase (labradorite type) and pyroxene augite. Magnetite is also a minor mineral. Secondary minerals are chlorite, sericite, calcite, and amphibole (tremolite- actinolite type). Mineralization is medium to high. Figure 4 and 5 show the microscopic images of the studied gabbro.

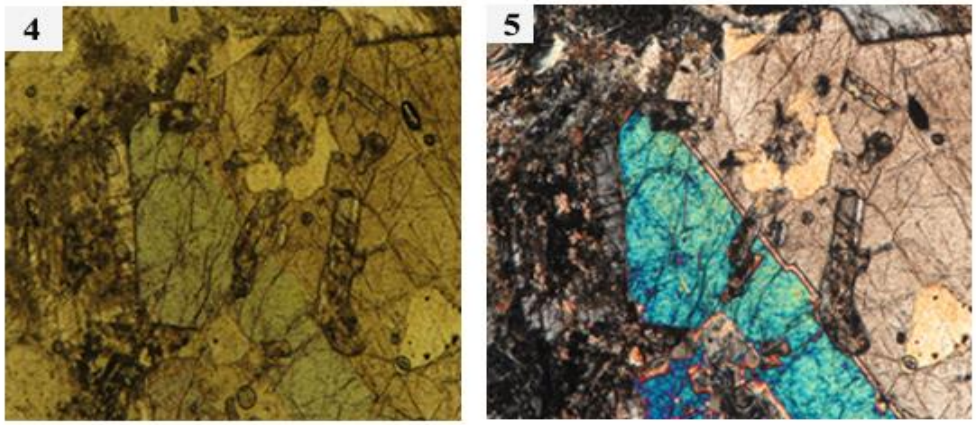


Figures 4 and 5- Microscopic images of a medium grained gabbro (Figure 4: PPL and Figure 5: XPL) [view field length: 4mm]

- Pyroxene gabbro

Medium grained pyroxene gabbro has a grain, poikililtic, Intergranular texture. The main minerals are augite and plagioclase (Labradorite type). Apatite is also seen in a needle shape as a minor mineral. Secondary minerals are chlorite stemmed from alteration of pyroxene augite, calcite and sericite which is altered out of plagioclase. Figure 6 and 7 show the microscopic images of this thin section.

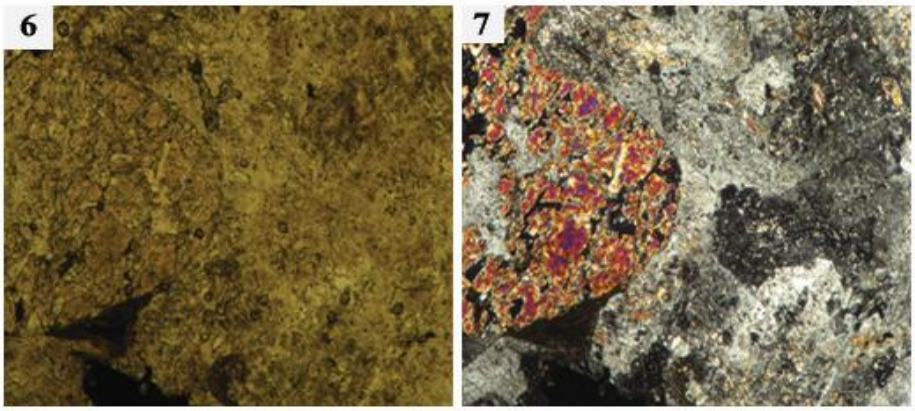


Figure 6-7: microscopic image of the studied pyroxene-gabbro (Figure 6: PPL-Figure 7:XPL; View field length: 4mm)

- Gabbro diorite

Gabbro diorite has a medium grained intergranular texture. Major minerals are plagioclase (labradorite type) and pyroxene augite. Minor minerals are biotite, apatite, opaque and chlorite. The latter mineral is stemmed from the alteration of augite. Mineralization intensity is medium. Figure 8 and 9 show the microscopic images of this thin section.

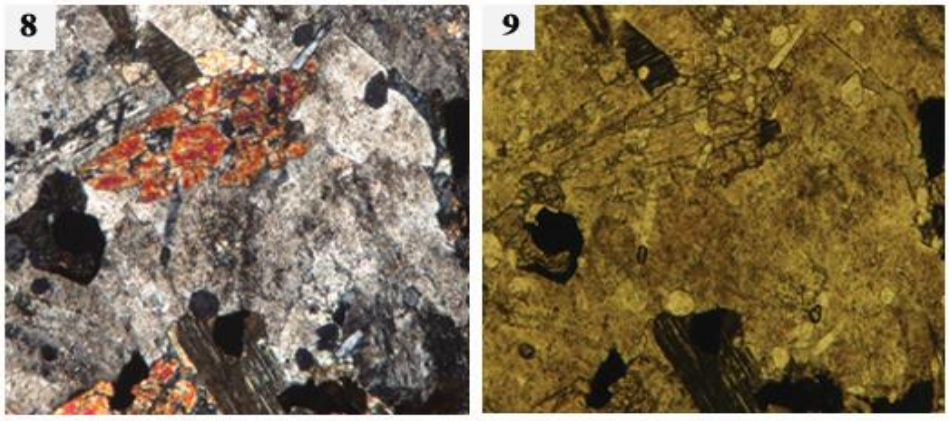


Figure 8-9: microscopic image of the studied gabbro-diorite (Figure 8: XPL-Figure 9:PPL; View field length: 4mm)

- Pyroxene diorite-gabbro

Gabbro diorite has a medium grained intergranular texture. Major minerals are plagioclase (andesine type with 48 percent anorthite) and pyroxene augite. Plagioclase types are saussuritized. The only minor mineral is opaque. Secondary minerals are amphibole, calcite, epidote, and chlorite. Mineralization intensity is medium. Figure 10 shows the microscopic image of this thin section.

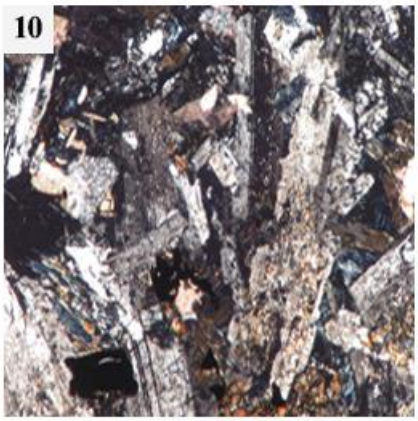


Figure 10: microscopic image of the studied pyroxene diorite-diorite (XPL, magnification rate: 40; View field length: 4mm)

- Pyroxene- diorite

It has a medium grained texture and plagioclase (andesine type) and pyroxene (augite type) are the major minerals. Opaque minerals include opaque. Secondary minerals are amphibole, calcite, tremolite-actinolite, epidote, chlorite and sericite. Alteration intensity is high in this rock. Figures 11 and 12 show microscopic images of the studied thin section.

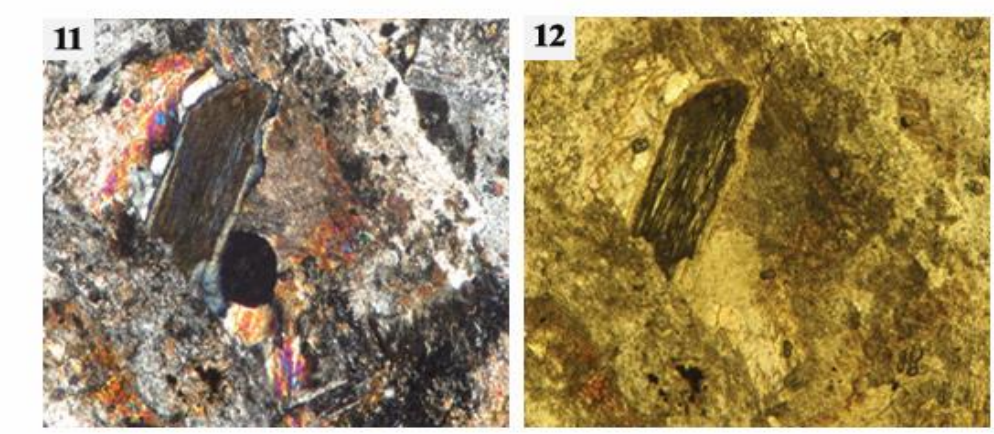


Figure 11-12: microscopic image of the studied pyroxene-diorite (Figure 11: XPL-Figure 12; PPL; View field length: 4mm)

- Diorite

Grained intergranular texture includes plagioclase (andesine type) and pyroxene (augite type). Minor minerals are opaque and apatite. Chlorite, calcite, epidote and uralite which are considered as secondary minerals. Alteration intensity is high and the microscopic images are shown by figures 13 and 14.

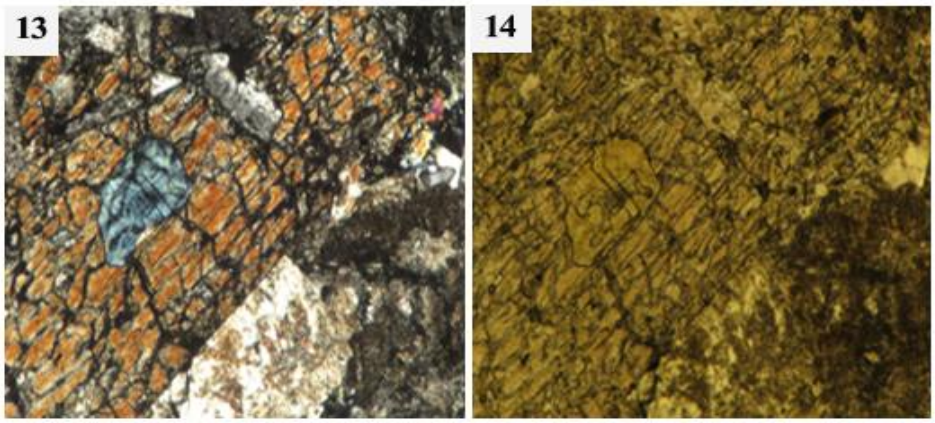


Figure 13-14: microscopic image of the studied diorite (Figure 13: XPL-Figure 14; PPL; View field length: 2mm)

- Loco-diorite

Medium grained intergranular texture has plagioclase (oligoclase to andesine type) and pyroxene (augite type) as major minerals. Secondary minerals are clino-zeolite, epidote, chlorite and calcite altered from plagioclase. Uralite and chlorite are also altered from augite. Alteration intensity is intermediate to high. Figures 15 and 16 show the images of the studied thin section.

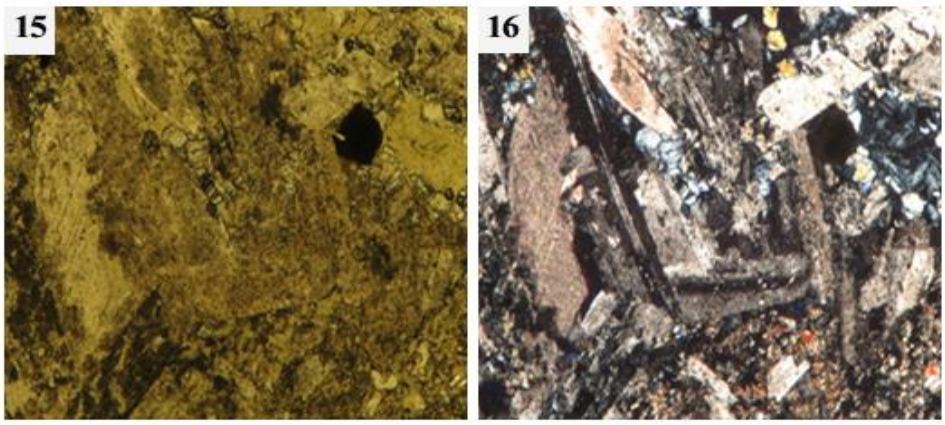


Figure 15-16: microscopic image of the studied loco-diorite (Figure 15: PPL-Figure 16; XPL; View field length: 2mm)

- Monzodiorite

Medium grained intergranular texture includes plagioclase and orthoclase as major minerals. Minor minerals are augite, apatite and opaque. Secondary minerals are also calcite, chlorite, sericite, epidote, and clino-zeolite. Alteration intensity is intermediate to high. Figure 17 and 18 show the microscopic images of this thin section.

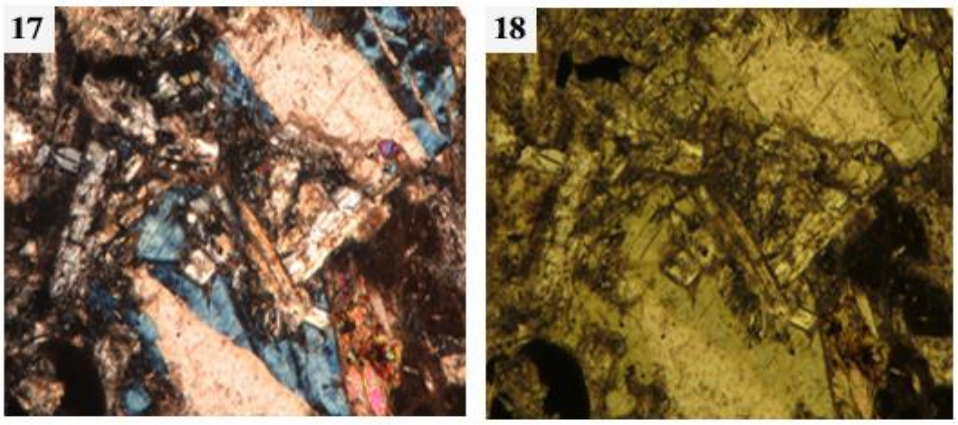


Figure 17-18: microscopic image of the studied monzodiorite (Figure 17: XPL-Figure 18; PPL; View field length: 4mm)

## 4. Streckeisen classification

The studied samples have been plotted on Streckeisen diagram. All the samples have been located in the regions 14 and 15. Region 14 includes monzodiorite and monzogabbro and region 15 consists of diorite, gabbro and anorthosite.

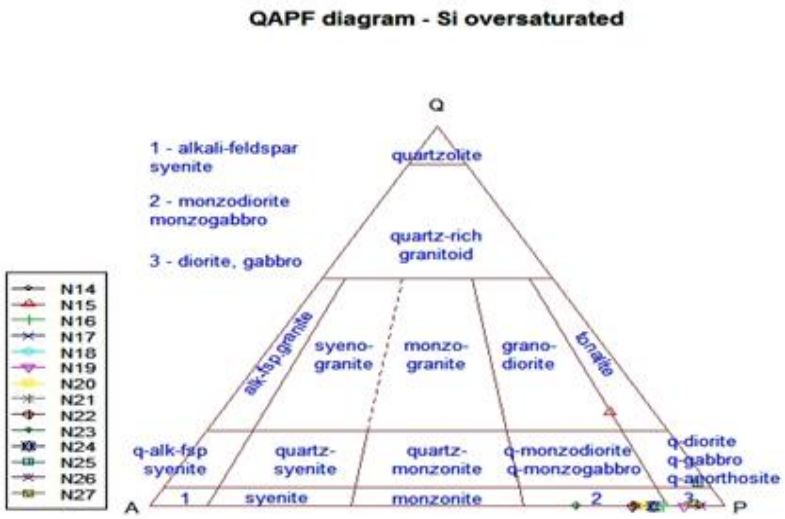


Figure 19- Location of the analyzed samples on Streckeisen diagram (Streckeisen, 1974)

## 5. Geochemistry

The geochemical studies have been carried out to determine the magmatic types and their origins.

### 5.1 TAS (Total Alkali Silica) diagram for plutonic rocks

TAS diagrams suggested by (cox etal, 1979), (Middlemost,1994) and (Middlemost,1985) is used for plutonic and volcanic rocks based on the geochemical contents raised by ICP analysis.

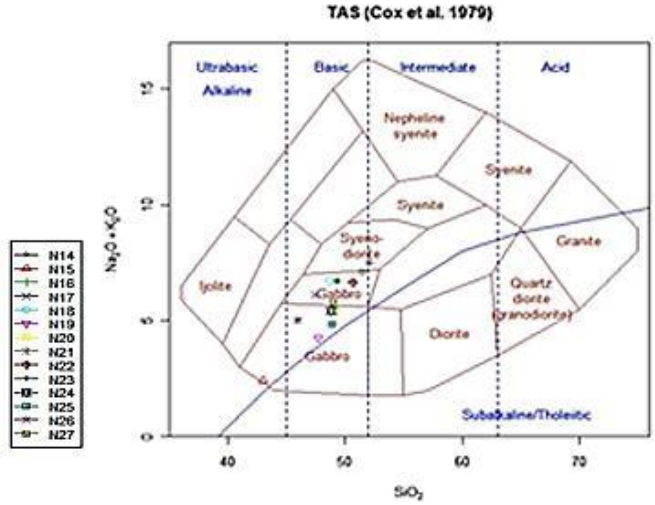


Figure 20- TAS diagram for defining intrusive rocks (Cox et al,1979)

According to TAS diagram for plutonic rocks, sample N15 is located on ultrabasic part and the rests are located on basic toward intermediate part, gabbro- syenodiorite. Also all the studied samples are located in alkaline part.

### 5.2 Diagram for Total Alkali vesus $SiO_2$ (Shervais 1982)

Based on the TAS diagram classifying all the samples as alkaline type, a distinctive diagram is used for determining the alkaline types of the samples. Based on figure 21, all the samples is located over the solid black line in the alkaline part.

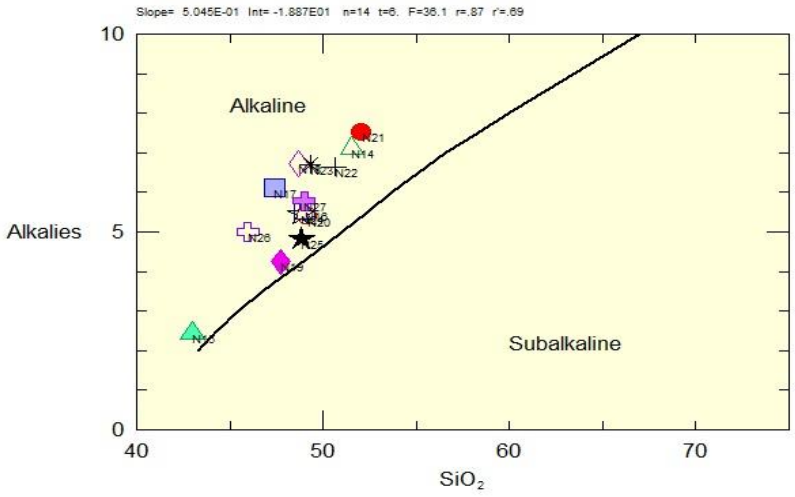


Figure 21- Total alkaline versus SiO2 (Shervais, 1982)

### 5.3 Total Alkali Silica diagram (Middlemost, 1994) for plutonic rocks

Sample N19 is plotted on gabbro part and N25 and N24 are plotted on monzogabbro part. The rests are plotted outside of this diagram.

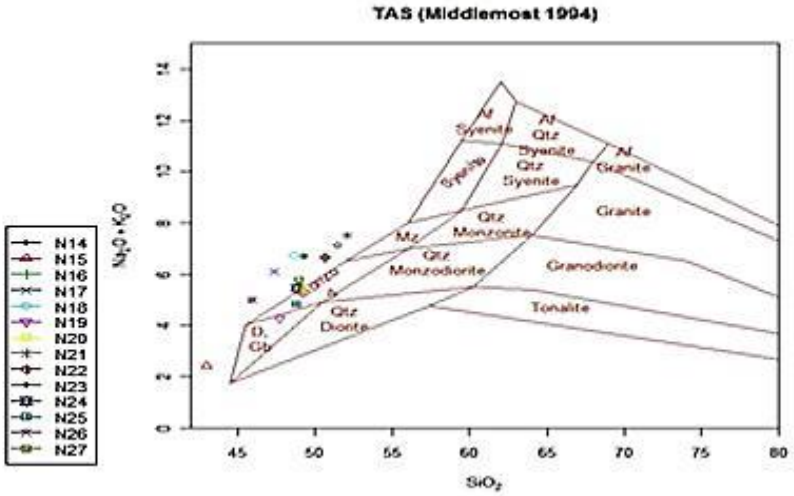


Figure 22- Diagram of defining intrusive igneous rocks based on TAS method (Middlemost, 1994)

### 5.4 De La Roche et al (1980) Cation diagram

This diagram is used for plutonic and volcanic rocks. It used cations in rocks calculating R1 and R2 and these parameters are plotted on X-Y.

Based on R1-R2 diagram, N19, N15, N25, N16, N24 and N20 are plotted on gabbro, monzodiorite, monzonite, alkali-gabbro, monzogabbro and syenogabbro, respectively. Rest of the samples are located on syenodiorite part.

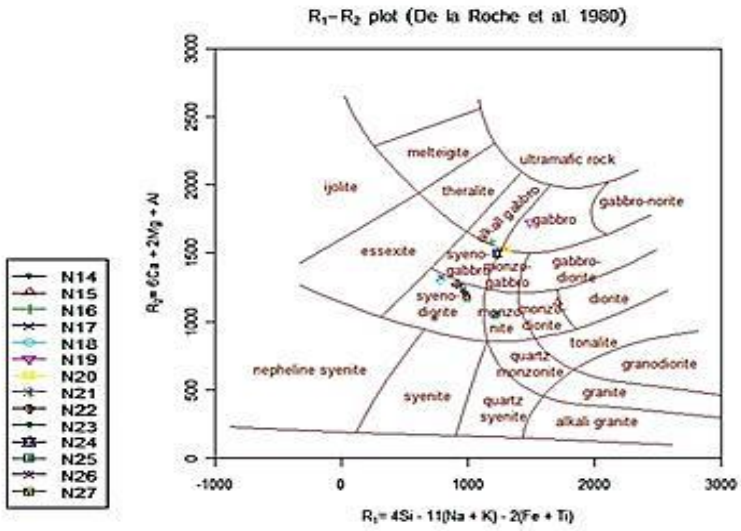


Figure 23- Determining the name of the intrusive igneous rocks based on the cations (De La Roche et al, 1980)

### 5.5 Peccerillo-Taylor 1976 diagram

This diagrams plots potassium versus silica giving rise to determining shoshonitic, high potassium calk alkaline, alkaline and low potassium tholeiitic series.

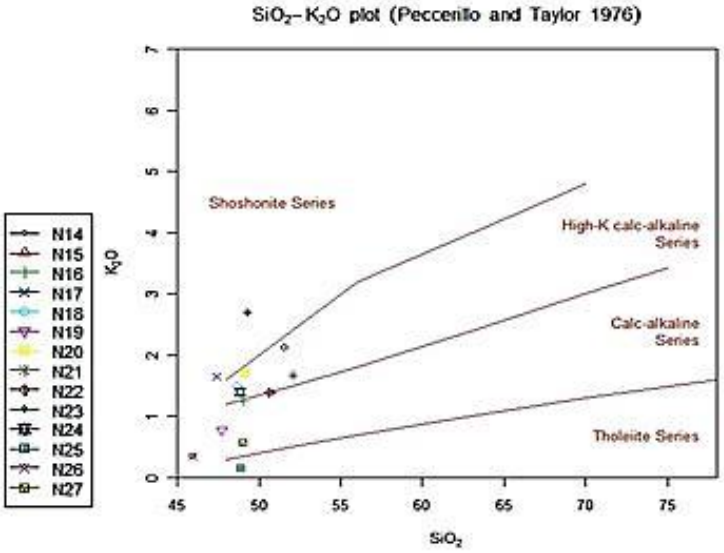


Figure 24- Peccerillo-Taylor 1976 diagram

According to Peccerllo-Taylor 1976 diagram, N25 has 0.16% K2O and it has lower content of potassium than other samples in the tholeiitic series. Having K2O equals to 2.7%, N23 has the highest content of potassium. Also N22, N27 and N19 have been classified in calk alkaline series and the rests are located in high potassium series.

### 5.6 Harker diagrams

Alfred haker, 1909 introduced a diagram in his book entitled natural history of igneous rocks. In this diagram SiO2 content (in X axis) is plotted versus major oxides (in Y axis). Figure 25 shows the Harker diagrams for the studied samples.

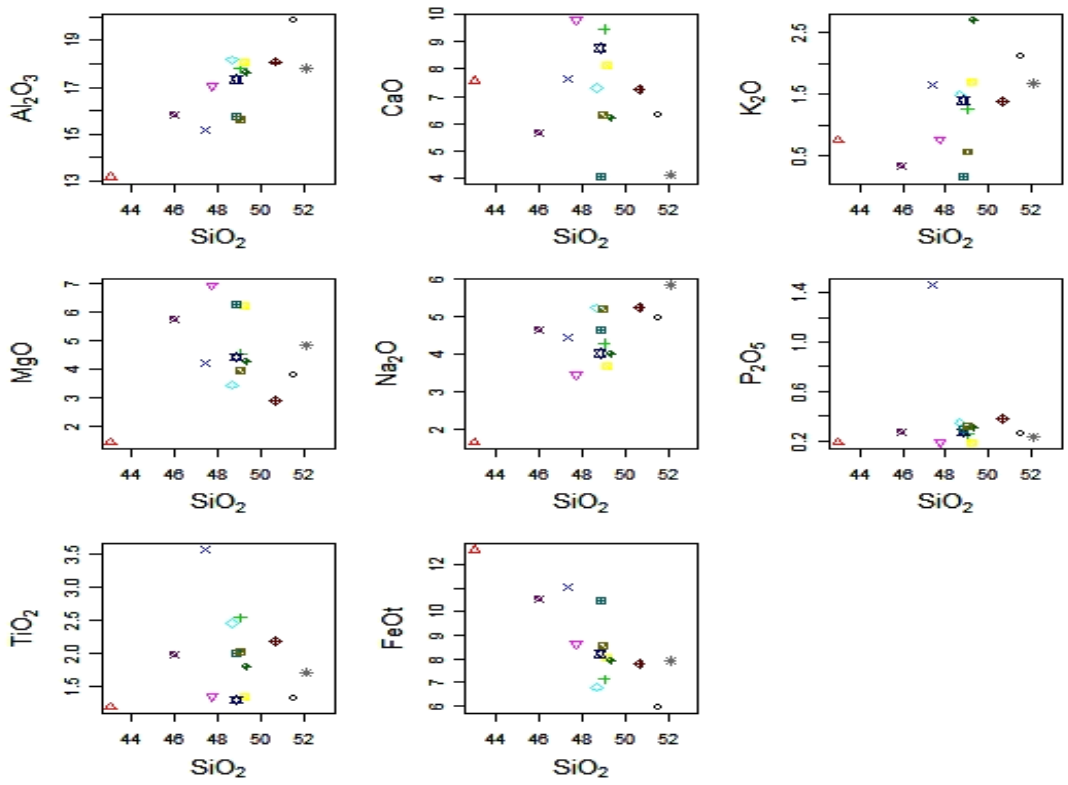


Figure 25- Harker diagrams (Major elements versus SiO2) (Harker, 1909)

CaO shows a decreasing trend versus SiO2 indicating a magma fraction and consumption of CaO in pyroxene, sphene, titanite, calcite and epidote.

FeOt shows a decreasing trend versus SiO2 indicating a fraction in the structures of opaque, pyroxene, and ilmenite minerals.

Based on K2O versus SiO2, the samples shows different genesis. Shoshonitic origin and high amount of potassium and calk tholeiitic minerals may have given rise to this anisotropic distribution.

Also, minerals containing potassium like alkali feldspar can be also detected in the thin section studies. The amount of potassium increases as SiO2 boosts in these samples. This trend might have been caused by remaining potassium in the last parts of magma fraction and its concentrating in feldspar phases.

MgO shows a decreasing trend against SiO2. Mg is a compatible element and its downward trend shows that the rock units bore high amount of the fraction process. Consequently, the rock units are far more away from their magma source. In the other word, a downward treand of MgO in the magma and fractional crystallization of olivine and olivine pyroxene happened simultaneously and amount of K2O and Na2O increase as well. Na2O shows an upward trend versus SiO2 and it is consumed in alkaline structure of feldspar and sodic pyroxene (acmite).

SiO2 and K2O increment and CaO and MgO reduction are responsible for magma fraction. In a nutshell, all the studied rocks have passed the magma fraction process.

### 5.7 Major elements versus MgO diagrams (Fenner diagrams)

Mg is considered as the most compatible element. It is also known as a key and identifier in geochemistry. Thus, major elements are plotted against Mg and lower amount of Mg can show a higher amount of fraction indicating studied rock is far away from its source. Based on MgO versus major elements, two different distributions and trends are observed revealing the fact that two different time spans are

responsible for the fraction or the rocks have been crystalized by a magma crystallization process but two different speeds.

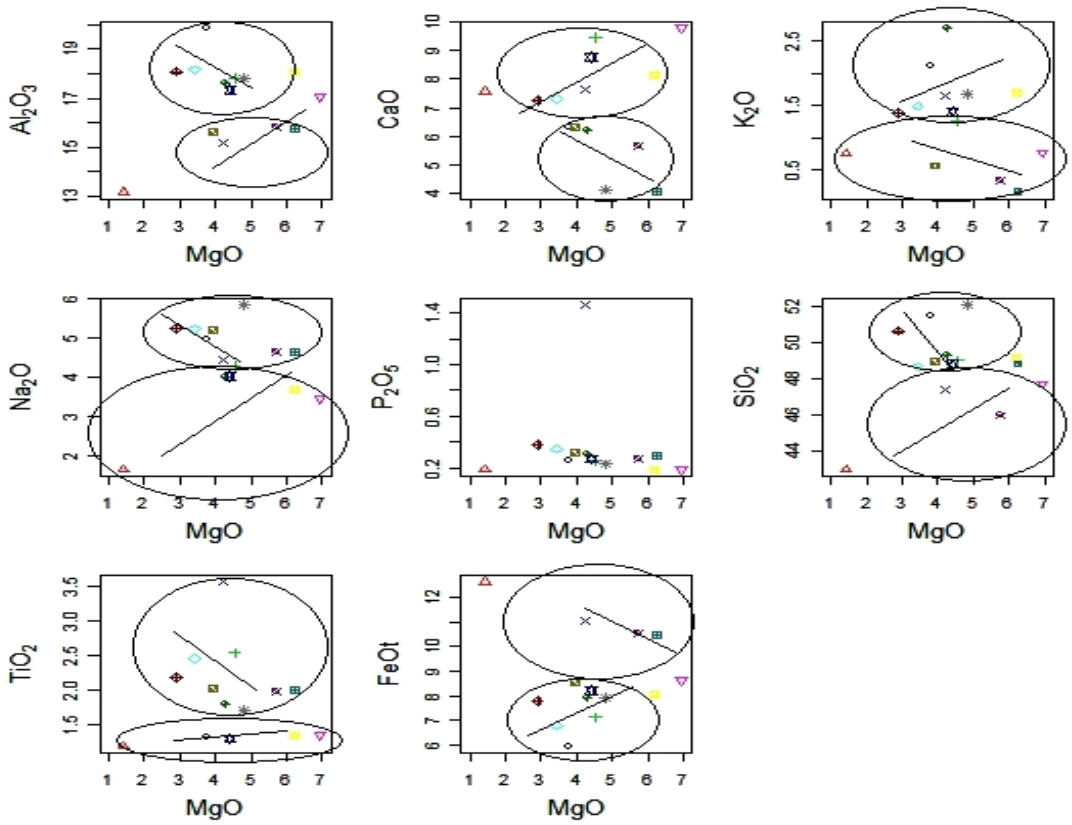


Figure 26- Diagrams of MgO versus Major elements (Fenner diagrams)

### 5.8 Spider diagrams

#### 5.8.1 Normalized to MORB spider diagrams

Large Ions Lithophile Elements, LILE, show concentrations of Th, K, and Rb. While, HFSE elements show depletion of P and Ti which can be related to low level of fractional melting of concentrated mantle (garnet lherzolite). Titanium based minerals show almost the same activities in the rate of solution decreasing as the pressure increases in fluids.

There is a slow negative slope in the spider diagrams from left to right. This fact together with their dendriticpattern (zig-zag shape) interpret the crustal contamination of these rocks (Wilson, 1989).

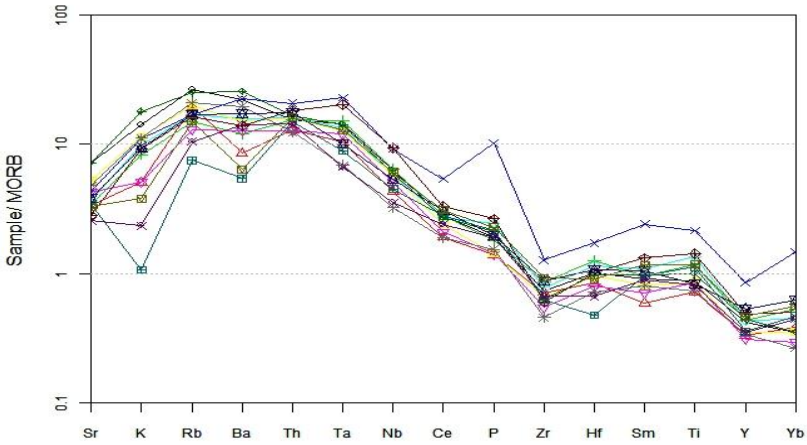


Figure 27- Spider diagram of REEs normalized to MORB (Pearce, 1983)

(LREE/MREE,HREE) Concentration is almost observed in all samples. The crustal contamination also results in positive anomalies in K, Th, and Rb.

### 5.8.2 Spider diagrams (normalized to chondrite) (Thompson, 1982)

Relative LREE concentration to MREE and HREE concentration is obviously high on all the samples. LILES concentration is also identified in the multi-elements spider diagrams normalized to chondrite (Thompson, 1982). The samples normalized to chondrite show positive anomalies for Ta, Th, and Sr. Sr enters feldspar crystalline and Rb is replaced in K-feldspar crystalline. Crustal contamination has also given rise to positive anomalies of K, Th, and Rb. Also, it is concluded that Ta, and Ti concentrations depend on ilmenite, rutile, and sphene. If these minerals decrease, Ti and Ta concentration may be related to minerals which have been remained in the magma source position. In this occasion these elements rarely enter liquids caused by fractional melting (Rollinson, 1993).

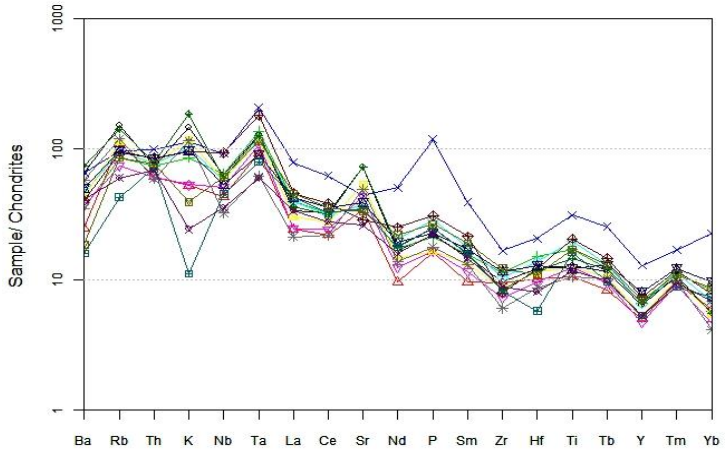


Figure 28- Normalized REEs to chondrite spider diagram (Thompson, 1982)

### 5.8.3 Spider diagrams of normalized REEs to chondrite (Boynton,1984.) & (Nakamura,1974)

LREE/HREE rates show a significant concertation. The concentration of LREE is a specification of OIB indicating presence of garnet in the magma source.

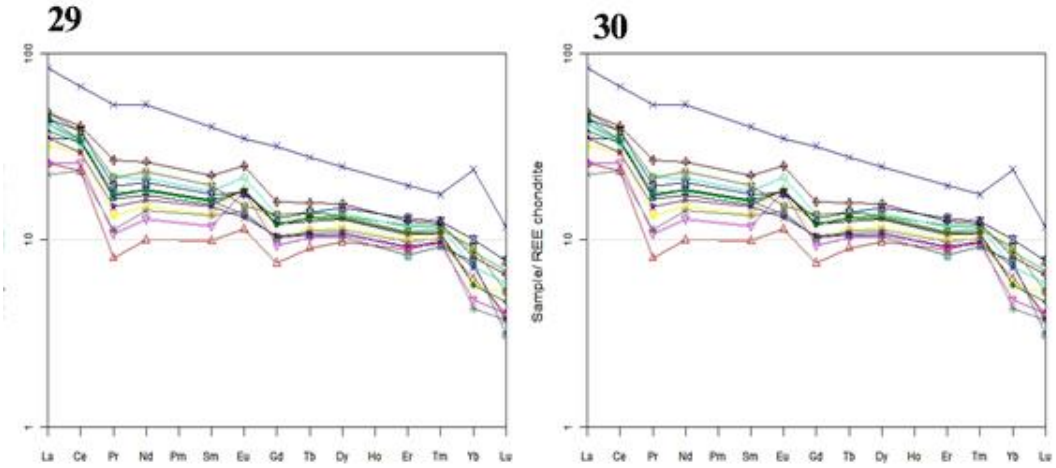


Figure 29- Spider diagram of normalized REEs to chondrite (Nakamura,1974)
Figure 30- Spider diagram of normalized REEs to chondrite (Boynton,1984)

There are two reasons put forward to explain the concentration of LREE in the studied samples:

1) LREEs are almost more compatible than HREEs. It might have happened due to low fractional melting in the source rock.
2) LREE concentration is one of the indications of magma with OIB source which can significantly explain the origins of the intrusive igneous rocks and geological history of the studied region.

Eu shows a positive anomaly in the spider diagrams of normalized REEs to chondrite. Early fraction and crystallization of plagioclase and olivine made Eu leave the magma and consequently remained Eu decreased in the magma of the studied rocks. In the other word, presence of plagioclase in the thin sections confirms positive anomaly of Eu.

It also can be concluded that Eu anomalies are usually controlled by feldspars since Eu (in two capacity state) is compatibale in calcium feldspar. While, other three capacity state REEs are incompatible with calcium feldspar. Thus, crystallization of calcium feldspar, whether it has been caused by fractional crystallization or fractional melting, resulted in negative anomaly of Eu. Eu shows a different pattern in two samples (N17 and N-17) demonstrating positive anomalies.

### 5.9 Triangle diagram of Y-Nb-Ce (Eby 1972)

Triangle diagram of Y-Nb-Ce is also used to confirm Ta-Yb (Pearce et al, 1984) diagram. The Y-Nb-Ce diagram consists of A1 and A2 parts. All the samples have been located in A1 part (Continental rift or intra-plate magma –related).

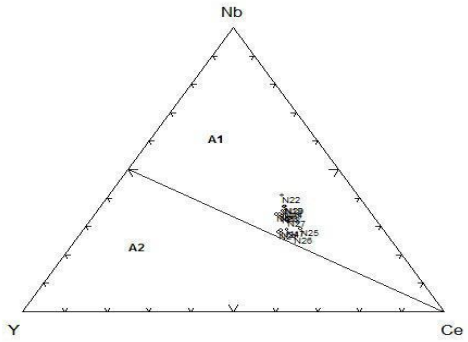


Figure 31- Triangle diagram of Y-Nb-Ce (Eby 1972)

### 5.10 Triangle diagram of (Nb*2-Zr/4-Y) (Meschede, 1986)

Base on Triangle diagram of (Nb*2-Zr/4-Y) (Meschede, 1986), the studied samples have been located in AI, AII=WP ALK (continental alkaline rocks) region.

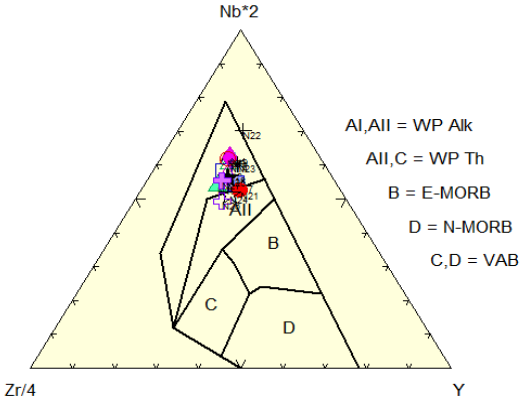


Figure 32- Triangle diagram of (Nb*2-Zr/4-Y) (Meschede, 1986)

### 5.11 Cabanis& Lecolle, 1989 diagram

It is concluded, based on this diagram, that all the rock units in the studied area have been located in the region of alkaline rifts with the continental crust.

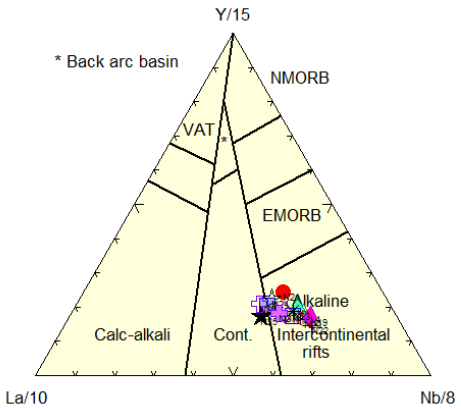


Figure 33- Determining the tectonic origins of the rock units (Cabanis& Lecolle, 1989)

## 6. Conclusion

Several outcrops of intrusive igneous rocks have been collected and studied in the region south and southeast of Arak toward north of Khomein (Markazi province, Iran). These outcrops are usually gabbro to monzodiorite. The rock types are gabbro, gabbro-diorite, diorite and monzodiorite. They are almost similar in their composition since their source magma was crystalized in almost similar state.

As far as mineralogy in concerned, several types of plagioclase minerals and pyroxene (augite type) could be identified in the region.

Based on the geochemical diagrams mentioned throughout the paper, all the samples have been located in basic to intermediate parts and most of the samples have been classified in alkaline and high potassium series and some others are classified as calk alkaline.

The primary magma had passed a little amount of fractional crystallization and crustal contamination producing rock units from gabbro to loco-diorite.

The diagrams also showed that the magma was produced by an intra continent alkaline rift. This tertiary continental rift caused a magmatism giving rise to make the injected magma. Significant similarities of the studied rocks can illustrate a huge gabbro-diorite batholith in the studied area (Between Arak and Khomein). Some outcrops of this batholite were observed and explored and sampled in some points due to erosion process.

## 7. References


Aghanabati, A. (2006). Geology of Iran, Geological Survey and Mineral Exploration. Country Publications, Tehran.

Boynton, W.V. (1984). Cosmochemistry of the rare earth elements; meteorite studies. In: Rare earth element geochemistry. Henderson, P. (Editors), Elsevier Sci.

Cabanis, B. & Lecolle, M. (1989). Le diagramme La/10-Y/15-Nb/8: Un outil pour la discrimination des series volcaniques et lamise en evidence des processus demelange et/ou de contamination crustale. Compte Rendus de l'Académie des Sciences Series II, 309, 2023-2029.

Cox, K. G., Bell, J. D.,& Pankhurts, R. J. (1979). The interpretation of igneous rocks. George Allen and Unwin., 450 pp.

De La Roche, H., Leterrier, J., Grandclaude, P., & Marchal, M.(1980). A classification of volcanic and plutonic rocks using R1R2-diagram and major-element analyses--Its relationships with current nomenclature: Chemical Geology, v. 29, p. 183-210.

Fenner, C, N. (1948). Incandescent tuuf flows in southern Peru. Geological society of America. Bulletin, V. 59, pp. 879-893.

Harker, A. (1909). The Natural History of Igneous Rocks. Methuen and Co., London.

Kholghi. M. H.(2004). 1:100K geological map of Varcheh and Khomein, Geological Survey of Iran.

Meschede, M.(1986). A method of discriminating between different types of mid-ocean ridge basalts and continental tholeiites with the Nb-Zr-Y diagram: Chemical Geology, Vol. 56, PP. 207-218.

Middlemost, E. A. K. (1985). Magma and magmatic rocks, An Introduction to igneous petrology. Longman Group U.K., pp. 73 – 86.

Middlemost, E. A. K.(1994). Naming materials in the magma / igneous rock system. Longman Groun u. k., 73 – 86.

Nakamura, N.(1974). Determination of REE, Ba, Fe, Mg, Na and K in carbonaceous and ordinary chondrites. Geochim Cosmochim Acta., Vol. 38, pp. 757-775.

Pearce, J.A. (1983). Role of the sub-continental lithosphere in magma genesis at active continental margins. In: Hawkesworth, C.J., Norry, M.J. (Eds.), Continental Basalts and Mantle Xenoliths, Shiva. Cheshire, UK, pp. 230-249.

Pearce, J.A., Harris, N.B.W., & Tindle, A.G.(1984). Trace element discrimination diagrams for the tectonic interpretation of granitic rocks: Journal of Petrology, v. 25, p. 956-983.

Peccerillo R.,& Taylor S. R. (1976). Geochemistry of Eocene calk – alkaline volcanic rocks from the Kastamonu area, northern Turkey. Contrib. Mineral. Petrol., V 58, pp. 63 – 81.

Rollinson, H. (1993). The Geochemistry of Mafic and Ultramafic Rocks from the Archaen Greenstone Belts of Sierra Leone.

Shervais, J. W. (1982). Ti–V plots and the petrogenesis of modernophiolitic lavas. Earth Planet. Sci. Lett. 59, pp. 101–118.

Streckeisen A.,& Le Maitre R. (1979). A chemical approximation to the modal QAPF classification of igneous rocks. Neues jahrb. Mineral Abh. 136, 169 – 206.

Thompson, R, N. (1982). British Tertiary volcanic province. Scoot. J. Geol., 18, pp. 49 – 107.

Vaezipour. M. J.(1985). 1:100K geological map of Varcheh and Khomein, Geological Survey of Iran.

Wilson, M. (1989). Igneous petrogenesis a global tectonic approach. Department of earth science, University of leeds. 466pp.